

## COMMUNICATIONS

# A Two-Dimensional Experiment That Separates Decoupling Sidebands from the Main Peaks<sup>1</sup>

Ēriks Kupĉe\* and Ray Freeman†<sup>2</sup>

\*Varian Inc., NMR Instruments, 36 Edgeway Road, Oxford OX3 0HE, United Kingdom; and †Jesus College, Cambridge University, Cambridge CB5 8BL, United Kingdom

Received December 4, 2000; revised April 11, 2001

**Broadband decoupling techniques generate undesirable cycling sidebands. The new two-dimensional technique described here allows separation of these sidebands from the main peaks by spreading the sideband responses in the indirectly detected dimension ( $F_1$ ) according to their frequency separations from the parent peaks, leaving the main resonances at zero frequency in  $F_1$ . This trace at zero frequency shows a thousandfold suppression of the residual sidebands, making possible the detection of very weak signals from dilute constituents of the sample. The experimental results can be displayed as one-dimensional “quiet decoupling” spectra without any significant loss of sensitivity. The new technique (DESIRE—decoupling sideband resolved spectroscopy) is simple, robust, and straightforward to implement.** © 2001 Academic Press

**Key Words:** cycling sidebands; sideband suppression; broadband decoupling; quiet decoupling; two-dimensional spectroscopy.

Modern broadband decoupling schemes involve the application of a *periodic* sequence of radiofrequency pulses, and as a consequence, the decoupled spectra always include some level of cycling sidebands that arise from residual pulse imperfections. Although numerous techniques for reducing sideband intensities have been suggested in the past (1–8), the degree of suppression is never perfect. This can be a major nuisance, particularly in biochemical studies where it is important to identify some extremely weak signals comparable in intensity with the cycling sidebands from much stronger responses.

We describe here a new two-dimensional experiment that separates decoupling sidebands from their parent peaks. A virtually sideband-free spectrum is obtained, suitable for the observation of the responses from very dilute species under investigation. The component of the total magnetization that gives rise to cycling sidebands is frequency-modulated, and this property is exploited to disperse the sidebands into the  $F_1$  dimension while the spectrum of interest appears on the trace at zero frequency.

The key to this new suppression technique is to allow the magnetization from the cycling sidebands to evolve during the  $t_1$  interval without any concomitant evolution of the magnetization from the parent peaks. This is achieved by a  $180^\circ$  pulse on the  $I$  spins that brings all chemical shifts to a focus at the end of the evolution period. Signal acquisition takes place during  $t_2$  under broadband decoupling conditions where both the parent and sideband signals evolve together.

The pulse sequence is shown in Fig. 1. Following the excitation pulse on the  $I$  spins, evolution of the heteronuclear spin–spin coupling ( $J_{IS}$ ) during the variable interval  $\Delta$  is refocused by the  $180^\circ$  pulse on the  $S$  spins. At the point where the  $J_{IS}$  coupling is fully refocused, a  $180^\circ$  pulse is applied to the  $I$  spins. The purpose of this pulse is to refocus the  $I$ -spin chemical shift evolution; it does not affect the evolution of the  $J_{IS}$  coupling. At this point, heteronuclear  $S$ -spin decoupling is switched on. During the following period  $t_1$  the frequency-modulated components of magnetization (the cycling sidebands) evolve and accumulate phase shifts that eventually determine the initial phases of the signals detected during the acquisition period. In complete contrast, the magnetization from the parent signals is refocused by the  $180^\circ$  pulse and starts the acquisition interval with zero phase shift, just as in a conventional pulse–acquire experiment. Consequently, in the resulting two-dimensional spectrum, only the cycling sideband frequencies appear in the  $F_1$  dimension while the parent peaks are all confined to the trace at  $F_1 = 0$ . Parent signals and decoupling sidebands both evolve during  $t_2$  so the sidebands are dispersed along diagonals that pass through the corresponding chemical shift frequencies on the trace  $F_1 = 0$ . Since the time-domain signals evolving during  $t_1$  have no imaginary parts, the spectrum is symmetrical about the line  $F_1 = 0$ , so the sidebands fall along two symmetrically related diagonals, reminiscent of those observed in “reflected” two-dimensional  $J$ -spectra (9, 10).

These doubly diagonal patterns of sideband responses are clearly evident in the two-dimensional spectrum of protons decoupled from carbon-13, shown in Fig. 2. The sample used for demonstration was a partially decomposed mixture of  $^{13}\text{CH}_3\text{I}$

<sup>1</sup> Presented in part as a poster at the 42nd Experimental NMR Conference, Orlando, FL, 11–16 March 2001.

<sup>2</sup> To whom correspondence should be addressed.

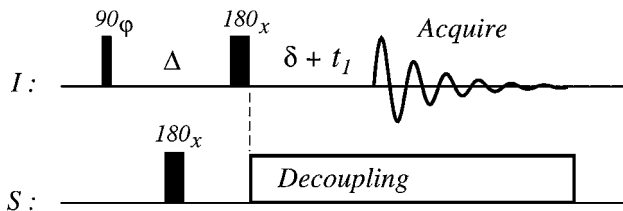


**FIG. 1.** Pulse sequence for separation of decoupling sidebands from the main peak. The duration of the delays on each side of the  $180^\circ(I)$  pulse are equal,  $\Delta = \delta + t_1$ . The fixed delay  $\delta$  is equal to or longer than the duration of the composite  $180^\circ(S)$  pulse. It can be used to adjust the phase of the strongest or closest sideband to reduce interference from the phase twist. Phase cycles:  $\varphi = -x, +x, +y, -y$ ; receiver  $+x, -x, +y, -y$ .

( $\delta_H = 1.95$  ppm,  $^1J_{CH} = 151$  Hz) and  $^{13}\text{CH}_3\text{P}(\text{O})(\text{OCH}_3)_2$  ( $\delta_H = 3.5$  and  $1.25$  ppm,  $^1J_{CH} = 129$  Hz), which contained a fair number of impurities. The protons of the methoxy groups are not coupled to carbon-13. The sideband-free “parent” spectrum runs along the trace  $F_1 = 0$ . Responses at nonzero frequencies in  $F_1$  represent the separations of sideband responses from their parent peaks. They allow any cycling sidebands that are only partially suppressed by the decoupling protocol to be properly identified. The trace at the top of Fig. 2 was derived from the first  $t_1$  increment of the two-dimensional experiment and represents the integral over all  $F_1$  values, showing all the normal residual sidebands.

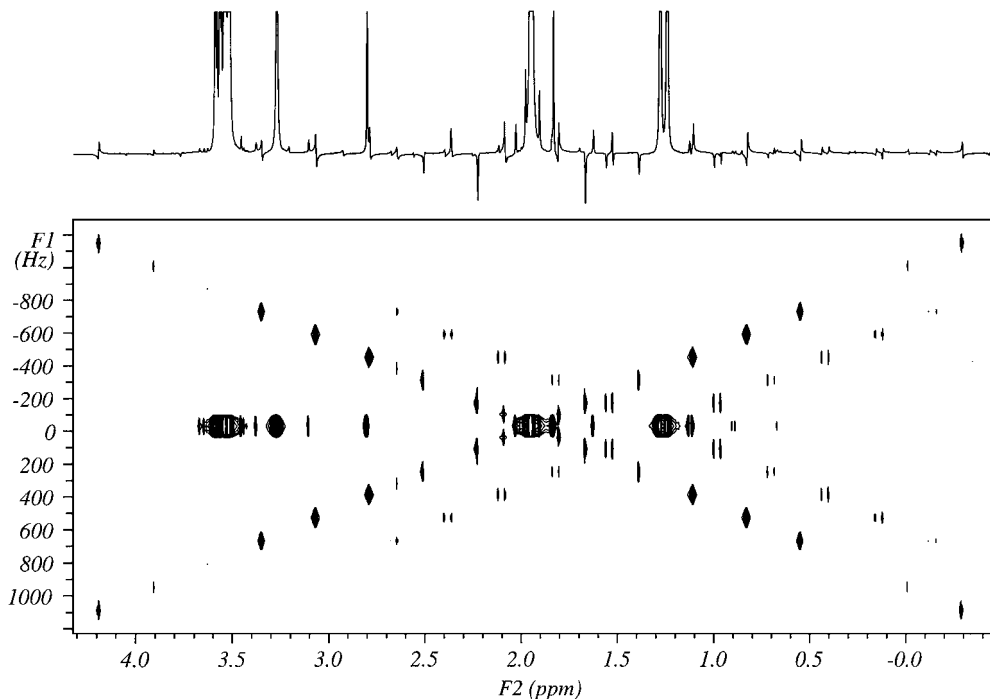


**FIG. 2.** The two-dimensional DESIRE spectrum of protons in a mixture of  $^{13}\text{CH}_3\text{I}$  and  $^{13}\text{CH}_3\text{P}(\text{O})(\text{OCH}_3)_2$  recorded at 500 MHz on a Varian INOVA spectrometer using GARP-1 decoupling of carbon-13. Only the responses at 1.25 and 1.95 ppm are coupled to carbon-13. The pulse sequence is shown in Fig. 1, with 128 increments, 4 scans per increment,  $\text{sw1} = 8928$  Hz,  $B_2(\text{max}) = 2.23$  kHz. A  $90^\circ(X)180^\circ(Y)90^\circ(X)$  composite pulse was employed as the  $180^\circ(S)$  pulse. The strongest sidebands, appearing at approximately 210 Hz from the main  $\text{CH}_3\text{I}$  peak (1.95 ppm), were phased by adjusting the delay  $\delta$  to 2.5 ms. The trace at the top shows the sidebands before suppression.

In Fig. 3 the main spectrum from a *decoupling sideband resolved spectroscopy* (DESIRE) experiment recorded using GARP-1 decoupling (9) is compared with a conventional GARP-1 decoupled spectrum. The sample is the same as that used in Fig. 2 and the tallest peak ( $\text{CH}_3\text{I}$ ) has been truncated at 2.5% in both spectra. A dramatic reduction of sideband intensity has been achieved.

The degree of sideband suppression in the DESIRE experiment largely depends on (a) the number of increments in  $t_1$ , (b) the length of the decoupling sequence, (c) the length of individual (composite) inversion pulses in the decoupling sequence, and (d) the overall stability of the spectrometer hardware. In order to minimize relaxation losses, the variable delays  $\Delta$  and  $t_1 + \delta$  need to be as short as possible. A high degree of sideband suppression can be achieved if  $t_1$  is set to an integer multiple of the duration of the decoupling cycle or supercycle. This corresponds to the requirement of “stroboscopic detection” in the theory of spin decoupling (11, 12). The optimum number of increments  $n_i$  is determined as

$$n_i = 2kmN, \quad [1]$$

where  $m$  is a positive integer, usually  $m = 1$ ,  $k$  is the number of phase cycling steps in the decoupling sequence, and  $N$  is a positive integer, a power of 2, that corresponds to the highest-order harmonic that needs to be eliminated (5, 6). The time increment

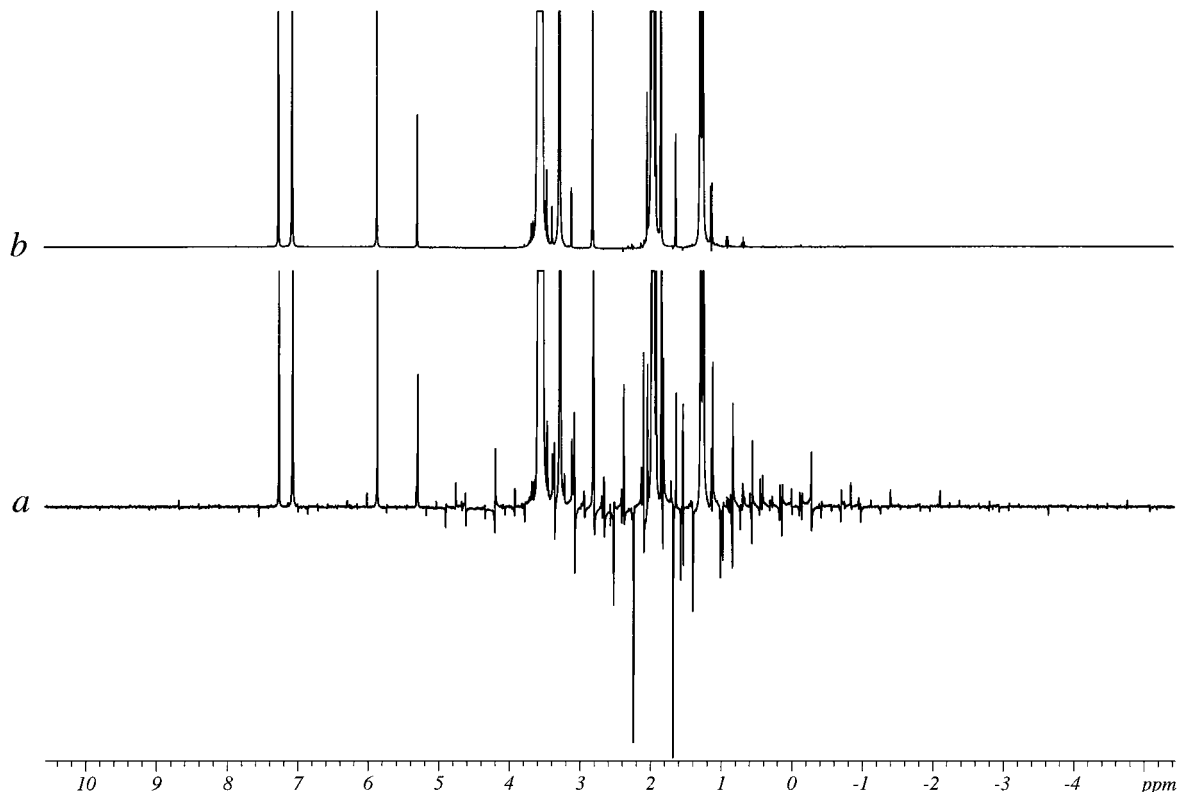


**FIG. 3.** Comparison of (a) the spectrum of the same sample acquired using conventional synchronous GARP-1 decoupling (128 transients) and (b) the corresponding DESIRE spectrum. Note the considerable reduction in cycling sidebands. Both spectra have been truncated at 2.5% of the tallest ( $\text{CH}_3\text{I}$ ) peak.

in  $t_1$  is calculated as  $T_d/(2N)$ , where  $T_d$  is the length of a single (composite) inversion pulse in the decoupling sequence. Note that subharmonic sidebands (5, 6) can only be eliminated if  $k$  is an even number. Hence decoupling sequences employing one of the iterative phase cycling schemes where  $k$  is an odd integer (13, 14) may require the number of increments to be doubled ( $m = 2$ ) to achieve optimum suppression of subharmonic sidebands.

Cycling sidebands that are closer to the parent line are more difficult to eliminate and require longer  $t_1$  evolution times. The inner sidebands (5, 6) are typically caused by a poor inversion profile of the basic  $180^\circ$  pulse in the given decoupling sequence, or because of inaccurate calibration of the radiofrequency field. Adiabatic pulses have the advantage of being less sensitive to radiofrequency calibration errors (15). It is essential that the effective bandwidth of the  $180^\circ(S)$  pulse be at least as wide as those in the following decoupling sequence. This can be achieved with either composite or adiabatic pulses (9). Alternatively, the same pulses that are used for the  $S$ -spin decoupling can also be employed for refocusing  $J_{\text{IS}}$ , as described earlier (7). This has the advantage of reducing some of the sidebands at the initial stage.

In addition to more conservative use of decoupling power, adiabatic decoupling (15) has the advantage of producing cycling sidebands fewer than those of conventional decoupling schemes,

giving a simpler DESIRE spectrum. The degree of sideband suppression achievable with adiabatic decoupling is shown in Fig. 4. A relatively long ( $T_d = 2$  ms) WURST-40 waveform (16) covering a 20-kHz bandwidth and phase cycled according to the MLEV-4 scheme (9) was employed to produce an extensive pattern of sidebands. This made genuine peaks in the spectrum from minor components essentially impossible to recognize (see Fig. 4a). We chose to suppress sidebands up to the fourth harmonic,  $N = 4$ . A considerable improvement of sideband suppression was obtained by applying a sine-squared window function in the  $t_1$  dimension. This required doubling the number of increments to  $n_i = 64$  ( $m = 2$ ). In order to minimize the subharmonic sidebands, a 1-ms constant adiabaticity WURST-40 pulse was employed as the  $180^\circ(S)$  pulse. A sideband-free spectrum obtained from the two-dimensional data set is shown in Fig. 4b. The vertical scale has been increased by a factor of 100. Only a few residual responses from the sidebands can be identified, the strongest of which is the eighth-order sideband marked by an asterisk (\*). Its intensity is only  $2.4 \times 10^{-5}$  of the main ( $\text{CH}_3\text{I}$ ) peak, demonstrating a remarkable suppression factor of 1000.

The two-dimensional version of this technique can easily be reduced to a one-dimensional "quiet decoupling" form by adding all the time-domain traces in the same memory location; the Fourier transform then gives the required trace at  $F_1 = 0$ . This

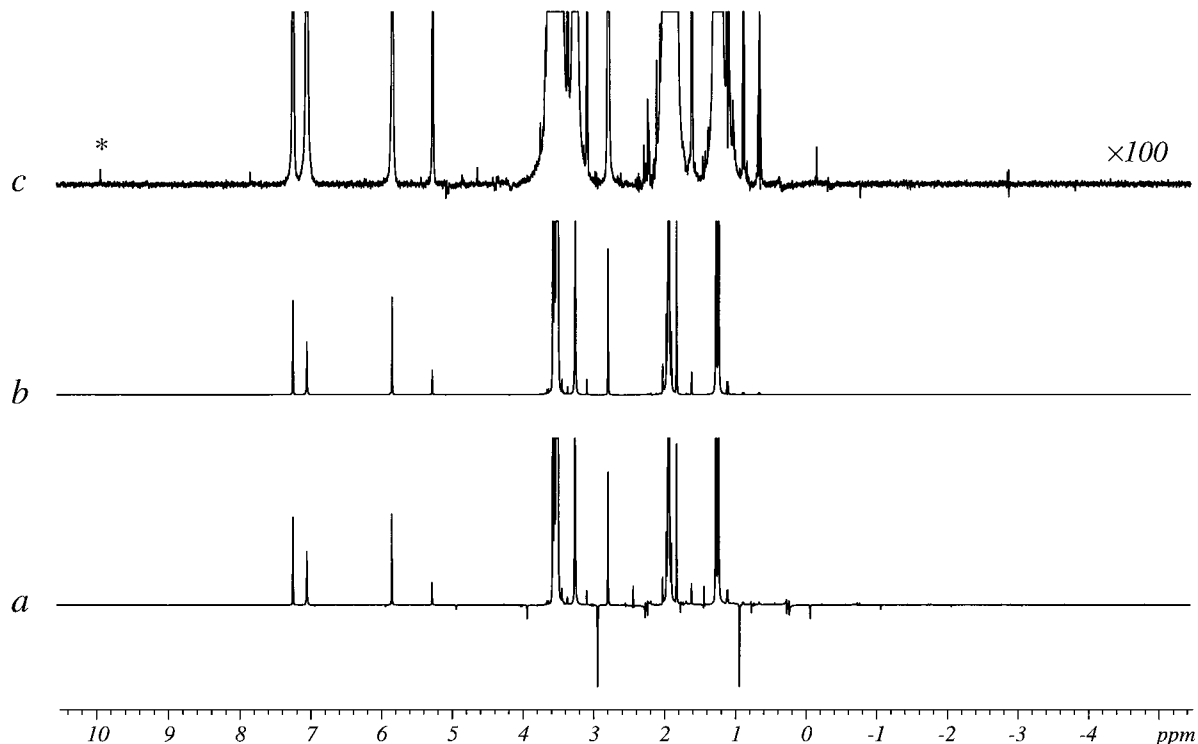


**FIG. 4.** Comparison of spectra of the same sample recorded employing adiabatic decoupling (WURST-40) with a 4-step MLEV phase cycle (9) and a WURST-40 defocusing pulse (7),  $sw1 = 4000$  Hz, 64 increments, 4 transients per increment, decoupling pulse length  $T_d = 2$  ms, decoupling bandwidth 20 kHz, adiabaticity factor  $Q = 2.5$ ,  $B_2(\text{rms}) = 2.31$  kHz,  $B_2(\text{max}) = 2.79$  kHz. (a) The Fourier transform of the first  $t_1$  increment, showing the cycling sidebands; the strongest is 2.4% of the parent (MeI) peak. (b) The DESIRE spectrum. (c) The same, with the vertical scale increased by a factor of 100. The strongest residual sideband is marked by an asterisk (\*) and is  $2.4 \times 10^{-5}$  of the parent signal, representing a 1000-fold improvement.

would also simplify the task of sideband suppression in more complex multidimensional experiments. The expected applications of DESIRE will normally involve dilute species requiring extensive time-averaging, so there would be no increase in total spectrometer time.

To conclude, the proposed technique allows an extremely high degree of sideband suppression in decoupling experiments and provides the means to identify any incompletely suppressed sidebands in the final spectrum. The new method should be useful for detection of minor components in spectra of high dynamic range. Apart from slight loss due to spin-spin relaxation during the short interval  $2\Delta$ , the sensitivity should be comparable with that of conventional one-dimensional spectroscopy, and in any case, for decoupled spectra of very dilute solutions, it is the residual cycling sidebands (rather than noise) that limit the effective sensitivity.

## REFERENCES

1. A. J. Shaka, J. Keeler, and R. Freeman, *J. Magn. Reson.* **53**, 313 (1983).
2. Z. Starcuk, Jr., K. Bartusek, and Z. Starcuk, *J. Magn. Reson. A* **107**, 24 (1994).
3. T.-L. Hwang, M. Garwood, A. Tannus, and P. C. M. van Zijl, *J. Magn. Reson. A* **121**, 221 (1996).
4. R. W. Dykstra, *J. Magn. Reson.* **82**, 347 (1989).
5. Ě. Kupĉe, R. Freeman, G. Wider, and K. Wüthrich, *J. Magn. Reson. A* **122**, 81 (1996).
6. Ě. Kupĉe and R. Freeman, *J. Magn. Reson.* **127**, 36 (1997).
7. Ě. Kupĉe, *J. Magn. Reson.* **129**, 219 (1997).
8. S. Zhang and D. G. Gorenstein, *J. Magn. Reson.* **147**, 110 (2000).
9. R. Freeman, "Spin Choreography," Oxford Univ. Press, Oxford (1997).
10. F. J. M. van de Ven, "Multidimensional NMR in Liquids," VCH, New York (1995).
11. J. S. Waugh, *J. Magn. Reson.* **50**, 30 (1982).
12. A. J. Shaka and J. Keeler, *Prog. NMR Spectrosc.* **19**, 47 (1987).
13. R. Tycko, A. Pines, and R. Gluckenheimer, *J. Chem. Phys.* **83**, 2775 (1985).
14. T. Fujiwara and K. Nagayama, *J. Magn. Reson.* **77**, 53 (1988).
15. R. Freeman and Ě. Kupĉe, *NMR Biomed.* **10**, 372 (1997).
16. Ě. Kupĉe and R. Freeman, *J. Magn. Reson. A* **115**, 273 (1995).